Modelling the Uranium-Hydrogen Reaction System for Tritium Storage

Ibrahim Salat

(Dated: November 24, 2022)

One of the main objectives of the International Thermonuclear Experimental Reactor, ITER, is to design a tritium storage facility that could sustain the high performance demand of the Tokamak. This paper reviews the usage of uranium to store tritium. Multiple models have been proposed to describe the reversible reaction between hydrogen and uranium, which have been analyzed in this paper. The paper proposes the idea of modelling the reaction using computational methods to better understand and predict the optimum storage conditions.

I. INTRODUCTION

The 1926 paper by Arthur Eddington proposes the idea that the sun generates its energy by nuclear fusion [1]. Using the idea of mass defect, the mass of an helium atom is less than the sum of the rest mass of its nucleons. Thus, the process of fusing hydrogen atoms to produce a helium atom in equation 1 is exothermic. The amount of energy released in fusion can be calculated by Einstein's energy equivalence equation $E = mc^2$. Ernest Rutherford, in 1934, was able to produce helium by fusing deuterium for the first time in a lab [2]. This led to the idea of fusion reactors to extract energy from the nucleus of an atom. Fusion energy is now considered the most suitable form of energy for the future as its benefits out weights any other form of energy. Fusion releases 4 million times more energy than burning fossil fuels, while having no toxic by-product [3].

$$ {}^{2}_{1}\mathrm{H}^{+} + {}^{3}_{1}\mathrm{H}^{+} \rightarrow {}^{4}_{2}\mathrm{He}^{2+}(3.6\mathrm{MeV}) + \mathrm{n}(14\mathrm{MeV}) \quad (1) $$

Initial research into fusion reactors began in the 1950's with the most popular design being the Tokamak. The Tokamak uses helical magnetic fields to confine and create a plasma of hydrogen isotopes. The plasma is an extremely hot mixture of positive ions and electrons that provide the right conditions for the fusion of deuterium and tritium to occur. The schematic of a Tokamak from the ITER facility is shown in figure 1.

Although any pair of atom with atomic mass less than iron can be fused to release energy, experimental data from figure 2 show that the biggest difference in binding energy per nucleon is between helium and tritium. Tritium is a radioactive isotope of hydrogen with an atomic mass of 3. It decays through beta emission, to produce a stable, noble gas, helium. Tritium is known as a soft beta emitter with the particles energy between 5.7 KeV to 18.6 KeV. The beta particle has a short range of about 6 mm and tritium has a half-life of 12.3 years therefore it is no harm to a human body [4]. Tritium and deuterium

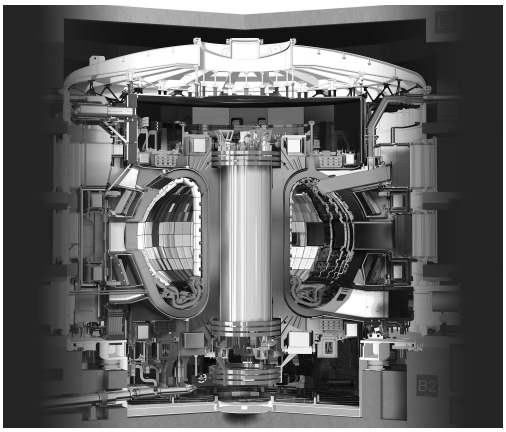

FIG. 1. The schematic of a Tokamak at the ITER facility. Taken from [3]

is used as fuels for fusion reaction not only because they release the most energy compared to any other elements but also because they reach fusion conditions at lower temperature and are very abundant to source.

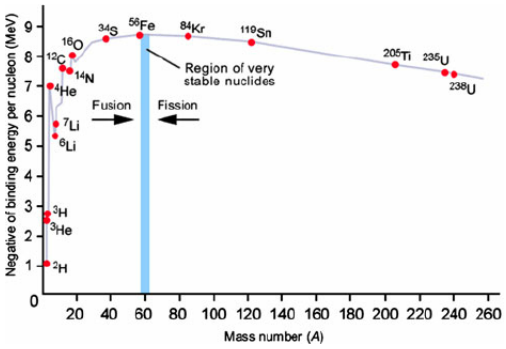

FIG. 2. Experimental data of BE per nucleon vs mass. Taken from [5]

Usage of tritium as a fuel, requires a fusion facility to have easy access to pure tritium. A significant objective of an international nuclear research project, ITER, is to design a storage bed that can meet the performance de-

mand required by the Tokamak [3]. This project deals with how tritium can be stored in a solid state form using uranium metal. It reviews, in detail the chemical reaction involved in the storage and the different models proposed to describe the reaction which would eventually be used to create a computation model. This computational model would be used to predict the initial parameters needed to have the optimum storage conditions.

II. URANIUM TO STORE TRITIUM

For a fully functioning nuclear fusion reactor, a tritium storage would be needed. One of the main problems with storing hydrogen for industrial purposes is its extremely low density, thus the solution should be a compact way to store hydrogen that makes it easy to transport and handle. There are multiple ways hydrogen can be stored. Hydrogen can be stored underground in salt mines in its gaseous form known as geological storage [6]. It can also be compressed or liquefied to store in storage units which requires high pressure or extremely low temperature and a suitable reservoir to sustain such extreme conditions. The most suitable way to store hydrogen and its isotopes for the purpose of fusion reactors is to store them as solid-states. A metal or a compound absorbs hydrogen by reacting with it under favourable conditions to form a hydride, and then de-absorbs hydrogen in other conditions. A large range of chemicals can be used for hydrogen storage, from simple metal hydrides to amides. Currently uranium is used to store tritium as uranium hydride in the UK [7].

Uranium is used because of the favourable characteristics of the reversable reation between uranium and hydrogen. Uranium-238 is abundant in nature, the operating hydriding temperature and pressure are not very high. The rate of forward reaction is almost equal to the rate of backward reaction and a highly pure hydrogen gas is released. The effects on the reaction when exposed to air and the reaction mechanism is well known and extensively studied. Uranium has the added advantage of operational benefits such as low thermal mass, high thermal conductivity and low equilibrium pressure [7].

$$2\mathrm{U} + 3\mathrm{H}_2 \leftrightarrow 2\mathrm{UH}_3 \tag{2}$$

Uranium hydride is formed by the reaction between gaseous hydrogen molecules and uranium crystals as in equation 2. The reaction is also known as corrosion of uranium as the resulting hydride is brittle, disintegrating the uranium metal, leaving behind a low density, toxic, pyrophoric, fine black powder [8]. Its lattice structure is very different from any of the three forms of uranium lattice structure which happen to be orthorhombic, tetragonal and body centred cubic. There are two phases of UH3, known as α-UH3 and β-UH3 and their formation is dependent on the temperature at the time of the formation of the hydride [9]. At below room temperature, the composition of the hydride is dominated by α-UH3, but with an increase in temperature the proportion of β-UH3 overtakes and at 200°C, almost all the uranium hydride is in β phase [10]. Both uranium hydride phases have a cubic lattice structure with different lattice parameters as shown in figure 3 . The more compact one being the α phase with $a = 4.142 \pm 0.002A$ and density, $11.55g/cm^3$. The beta phase has a lattice parameter of $a = 6.625 \pm 0.003A$ and density $11.29g/cm^3$ [11]. In both phases each uranium atom is surrounded by 12 hydrogen atoms but there are 2 uranium atoms in each primitive cell in the α phase and 8 uranium atoms in the β phase. The formation of UH_3 is exothermic as the heat of formation is recorded to be $-129.8kJ/mol$ [12].

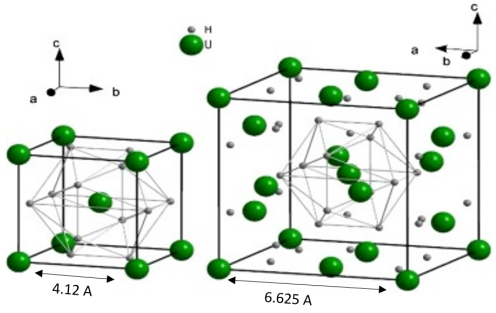

FIG. 3. Lattice Structure of α (left) and β (right) uranium hydride. Adapted from [8]

III. THE THEORY

A. Overview

Figure 4 shows an ideal pressure vs time graph for the reaction between uranium and hydrogen and indicates that the reaction takes place in 4 different stages [8].

The Induction Period - Uranium metal very readily forms an oxide upon exposure to air. It is very difficult to not have an oxide layer on the surface of the uranium metal when making uranium hydride using equation 2. The presence of an oxide layer means that the hydrogen needs to first diffuse through it before it can attack the metal [13] which is only possible if the concentration of hydrogen is higher than its solubility limit of $0.03 - 0.04\mu g(H_2)/g(UO_2)$

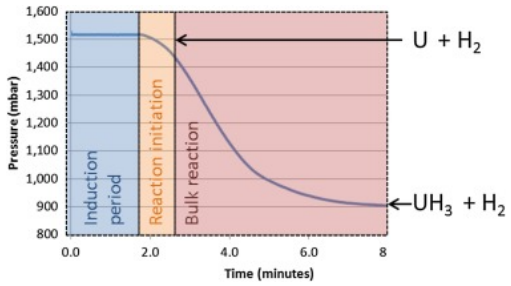

FIG. 4. Ideal reaction pressure-time graph indicating the 4 stages of the reaction. Taken from [8]

.

[14]. The induction period is considered to be from the start of the reaction to the first appearance of the first nucleation growth spot. One of the factors that affect the induction period is the form of uranium metal used. In the case of storage for a fusion reactor the uranium is in fine powder, which has been shown to reduce the induction period or completely remove it [15]. This is because of the high surface area to volume ratio, that not only increases the reactive surface but also increases the heat released thereby increasing the reaction temperature.

Reaction Initiation - It is a widely accepted fact that the reaction commences with individual reaction spots on the metal surface although some observation suggests that the reaction usually starts with one spot at first then other spots appear until the reaction spreads over the whole metal surface [16]. Each nucleation spot tends to grow downwards into the metal and laterally [16]. Under desired conditions, the rate of spot formation is very high, but this is affected by environmental factors such as the purity of the hydrogen gas and the presence of an oxide layer. For the reaction to reach saturation point, that is when the increase in nucleation spots has stopped and covers about 7 to 10 percent of the surface [17], the influx of hydrogen to the surface have to be greater than the rate of hydrogen diffusion into the bulk metal [8].The spots then tend to grow radially and merge to cover the whole surface.

Bulk Reaction - Once the reaction reaches the saturation point, it covers the surface of the metal forming a reaction front that travels into the bulk material with velocity V_s . This is the region where most of the reaction takes place hence a decrease in hydrogen pressure in figure 4. The models discussed later in the paper aims to model this part of the reaction by predicting the spall velocity V_s [18].

Equilibrium - Once 70 to 80 percent of the bulk uranium has been converted to uranium hydride and the rate of forward reaction is equal to the rate of back reaction, the reaction system reaches a state of equilibrium hence explaining the plateau at the end of the curve in figure 4 and completing the 'S' shaped curve.

B. Bloch-Mictz Model

In the 1981 paper [19], Bloch and Mintz (BM) propose two possible models to explain the reaction mechanism of uranium and hydrogen:

Diffusion through the protective product layer - The product forms a barrier, reducing the penetration of the hydrogen gas to the metal surface. As the reaction carries on, the product layer starts to deplete, as a result the apparent product layer remains a constant thickness due to the balance between depletion and production of the product layer.

Interfacial growth: The product layer is assumed to be easily penetrated by the gas therefore the rate limiting step is the reaction at the surface of the metal. Bloch and Mictz perform hydriding experiments to compare the data to the two models proposed. The first models fit well in the high pressure range of the experiment but don't perform well in the low pressure region. BM use the 2nd model to propose the following equation to model the reaction mechanism between uranium and hydrogen.

$$u_{\mathrm{g}} = K_{\mathrm{eq}} \left\{ \left(\frac{P}{P_{\mathrm{d}}} \right)^{n/2} \left(\frac{1 + K_{\mathrm{m}} {P_{\mathrm{d}}}^{1/2}}{1 + K_{\mathrm{m}} P^{1/2}} \right)^{n} - \left(\frac{P_{\mathrm{d}}}{P} \right)^{m/2} \right. \tag{3}$$

$$K_{\mathrm{eq}} = k_{\mathrm{d}} {K_{\mathrm{h}}}^{-m} P_{\mathrm{d}}^{-m/2} \tag{4}$$

Equation 3 gives the hydride growth rate U_{g}, using 4 parameters, equilibrium rate constant - k_{m}, hydrogen pressure - P, equilibrium pressure P_{d} and k_{eq} given by equation 4.The constants m and n are the number of available or occupied hydrogen sites in the uranium lattice needed for a phase change, respectively.

C. The Condon Kirkpatrick Model

The Kinetics model proposed by condon and kirkpatrick (CK) predicts the rate of hydride formation as a function of hydrogen pressure and the temperature of the reaction [20]. The reaction between uranium and hydro-

gen is made up of different rates, condon's model successfully predicts the constant reaction rate stage [21] whereas Kirkpatick's solutions to condon's model consider other stages of the rate reaction, giving a more accurate representation of rate when compared to experimental data [22].

The CK model expresses the hydriding rate as either weight gain rate, $w\dot{g}(t)$ or the spall front velocity, V_s [23]. The spall front velocity is the speed of the moving boundary between the reaction product and the unreacted uranium metal.

The CK model provides a set of following differential equations, using Flicks second law of diffusion with a sink term that describes the reaction:

$$\frac{\partial C}{\partial t} = \frac{\partial}{\partial x}\left(\frac{DN}{N-C}\frac{\partial C}{\partial x}\right) + s\frac{\partial U}{\partial t} \tag{5}$$

$$\frac{\partial U}{\partial t} = -k_1\left(C - C_{\text{eq}}\right)U + k_2(1-U)^{1/3} \tag{6}$$

C is the concentration of hydrogen in the metal, D is the diffusivity constant, N is maximum amount of hydrogen the uranium lattice can hold, U is the reacted uranium molar fraction and k_1 and k_2 are the rate constants.

Equation 5 is a diffusion equation with the sink term - $s\partial u/\partial t$, where s is the stoichiometric constant - 3, Whereas, equation 6 consists of the hydriding and dehydriding rates constants. The initial conditions are set to make the concentration of Hydrogen gas at at the start of the reation to 0, $C(x,0) = 0$ and the unreacted molar fraction of uranium to 1, $U(x,0) = 1$. One of the features of this model is the assumption that any fraction of $U < U_{\text{c}}$ has broken away from the metal, giving one of the boundary conditions, $U\left(x_{\text{C}},t\right) = U_{\text{C}}$. Another assumption made was that the product is finely divided powder and has hydrogen concentration of C_0 leading to the other boundary condition, $C(x_c,t) = C_0$

Combining the 2 boundary conditions, it can be seen that the condition U$< U_c$ applies in the region between the surface and spall front. In that region, the concentration remains the same as described by the boundary condition and the hydriding and dehydriding occur with $C = C_0$ in eq 5.

The finalized CK model is a product of multiple modifications to the original model proposed by condon [24][22][21][25]. Equation 5 can be used to solve for the spall onset time t_I by integrating:

$$\int_{U=1}^{U=U_c} \frac{dU}{-k_1C_0U + k_2(1-U)^{1/3}} = \int_{t=0}^{t=t_I} dt = t_I \tag{7}$$

Rewriting the left hand side of the equation in a cubic form gives an important parameter α, the ratio of dehydriding to hydriding [23].

$$\alpha \equiv \frac{k_2}{k_1C_0} > 0 \tag{8}$$

The spall speed, V_s can then be calculated using the following equation [21]:

$$v_s(P,T) = \frac{1}{t_I}\sqrt{\frac{D_E}{3k_1\sqrt{U_c}}} \tag{9}$$

D_e is the effective hydrogen difusivity in uranium defined by:

$$D_e = \left(1.9\times10^{-6}\frac{\text{m}^2}{\text{s}}\right)e^{-(5820\text{ K})/T}\sqrt{\frac{N}{N-C_0}} \tag{10}$$

In 1993, Powell [25] modified the equations given by the original CK model to better fit experimental data given by Wicke and Otto in [26]. The modifications are given in table 1. The general weight gain equation can then be given by equation 11

$$w\dot{g}(t) = 8.00\times10^4\left\{3v_s\left(1-U_{\text{stop}}\right)\right. \left[1-U_ce^{-k_1C_0(t-t_l)}\right] + C_0v_s \tag{11}$$

Where $w\dot{g}(t)$ is the weight gain, c_0 is the concentration of hydrogen in uranium at equilibrium and U_{stop} is the reacted uranium mole fraction at equilibrium.

D. The Shrinking Core Model

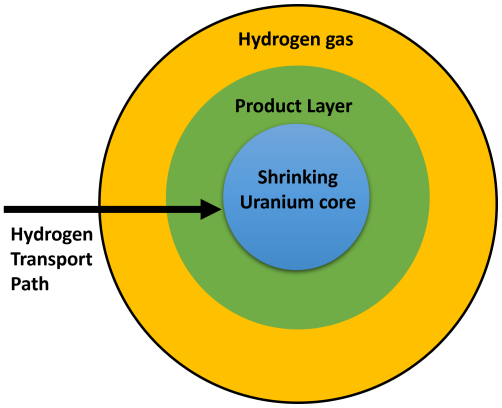

FIG. 5. Shrinking core model of the formation of uranium hydride.

Parameters	Original CK	CK Powell
D_e	$\left(1.9 \times 10^{-6} \frac{\mathrm{m}^2}{\mathrm{s}}\right) e^{-(5820\ \mathrm{K})/T} \sqrt{\frac{N}{N-C_0}}$	$\left(1.9 \times 10^{-6} \frac{\mathrm{m}^2}{\mathrm{s}}\right) e^{-(5820\ \mathrm{K})/T}$
N	$e^{-2.362-[(2305\ \mathrm{K})/T]}$	$N_{93}(T) = e^{-1.42-[(2783\ \mathrm{K})/T]}$
U_c	$1-(1-0.989)^{0.5-0.5\tanh\{4.307-[(2950\ \mathrm{K})/T]\}}$	$1-(1-0.995)^{0.5-0.5\tanh\{3.6425-[(2500\ \mathrm{K})/T]\}}$

TABLE I. The table shows the parameters modified by Powell in 1993 [25].

The shrinking core model was proposed in [27] which considers the the shape of the uranium metal to be a small pellet as shown in figure 5, obtained by powdered uranium by dehydriding uranium hydride [7]. The core of the pellet is the uranium metal and the outer layer is the product of the reaction. Rc is the radius of the core which is equal to R, the radius of the pellet, at the start of the reaction. The reaction begins as the core radius decreases from R to Rc then to finally 0 at the end of the reaction. The product formed usually falls off, but this model assumes that the product remains intact with the core. Due to the difference in the densities of uranium and uranium hydride, the outer layer increases in thickness. The outer layer is considered porous to the hydrogen gas while the core is not permeable, so the reaction happens at the surface of the core. The temperature of the pellet and the gas is also assumed to be the same through out the reaction.

The relation between the pellet initial diameter, the diameter at time t and the unreacted uranium is given by:

$$R(t) = \left[\left(R^3 - r_c^3\right)\frac{\rho_U}{\rho_{UH3}} + r_c^3\right]^{\frac{1}{3}} \qquad (12)$$

Where ρ_u is the density of uranium and ρ_{UH3} is the density of uranium hydride.

IV. DISCUSSION

Multiple models and modifications have been proposed to accurately predict the nature of the reaction [28], each trying to optimise the model parameters that fit the empirical data. Condon-Kirchpatrich and B-M models have been more accurate in predicting experimental data than other models such as the WO model [26], because they consider the hydrogen solubility limit along with hydrogen solubility in uranium metal. BM do this by setting up the boundary condition that at equilibrium pressure the rate must go to zero and CK do this by incorporating hydriding and dehydriding functions.

Comparing the 2 models in consideration reveals that the BM model consistently predicts values of linear rate 2 to 3 times lower than the Ck model and has a peak at 50 degree higher than the CK model as shown in figure 6 [29][23]

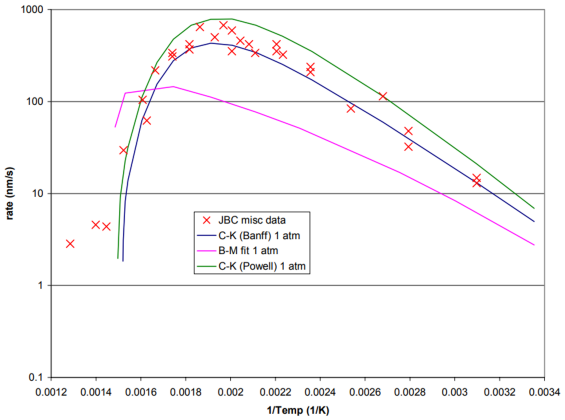

FIG. 6. comparing the rate-time graphs of the 2 models. taken from [29]

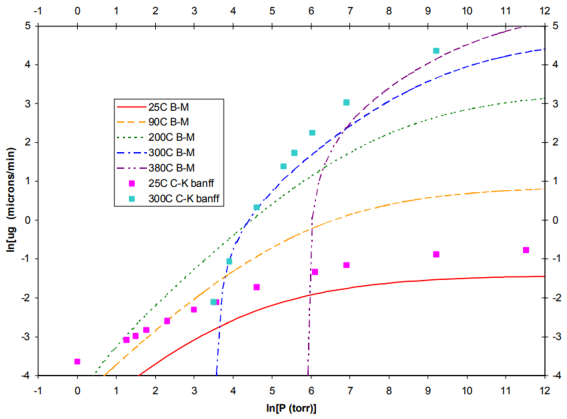

FIG. 7. Comparing the pressure-time graph of the 2 models. taken from [29]

Comparing the linear rate vs pressure graph between the the CK and BM model also show that CK model predicts higher values as shown in figure 7. The Ck bnaff model is the original CK model and the CK powell model is the modified CK model. The original CK model fits the data the best but that is because the model was fine tuned to fit the empirical data so it is no surprise it fits the best. One of the major modification of powell was the modified equilibrium pressure as a function of temperature

which has been compared in figure 8 against the original ck model.

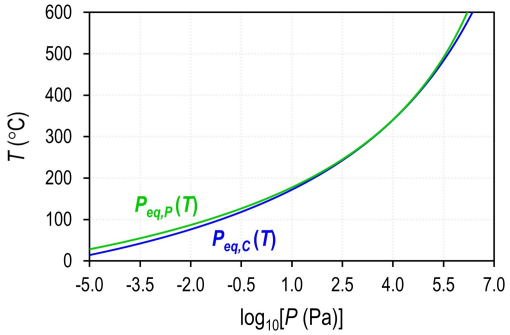

FIG. 8. Pressure-time graphs showing the difference in modified linear rate CK model in green and the original CK model in blue. Taken from [23]

Future work - The aim of the project is to build a working computational model using the above-mentioned models to accurately predict the behaviour of the reactants and product with change in storage parameters. For fusion reactors, tritium is stored using powdered uranium, which is made using 5 to 6 cycles of hydriding and dehydriding the uranium metal. This means that the shrinking core model would be best suited to base the model on. The model mentioned above only considers one single pellet, therefore further investigation would be needed to understand their bulk behaviour. The shrinking core model also assumes the protective barrier model proposed by bloch which was then shown to not produce accurate results. Therefore Our final model should adapt the shrinking core model with Bloch's interfacial growth model and the modified CK powell rate equations. Once a base model is achieved then other external factors need to be taken into account such as effects of an oxide layer which can be reduced depending on the handling of the metal before the reaction commences. Eventually our model should be able to reproduce the results in figure 9 from paper [7].

V. CONCLUSION

Research into fusion reactors have been going on since the 1950's, and a significant amount of research has been done on the corrosion of uranium. The 2 main models proposed in the last 65 years have been reviewed in this article. Since the reaction mechanism is still not completely understood, a computational model needs to be made that would help predict the optimum parameters for tritium storage.

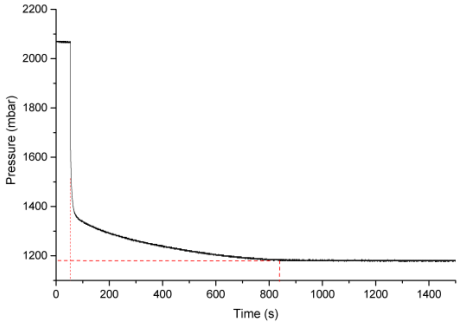

FIG. 9. Experimental pressure time graph from [7]

REFERENCES

1. *Arthur S. Eddington, The Nature of the Physical World: Gifford Lectures of 1927, An Annotated Edition - Cambridge Scholars Publishing* [Online; accessed 19. Nov. 2022]. Nov. 2022. https://www.cambridgescholars.com/product/978-1-4438-6386-5.
2. Oliphant, M. L., Harteck, P. & Rutherford. Transmutation Effects observed with Heavy Hydrogen. *Nature* **133,** 413. ISSN: 1476-4687 (Mar. 1934).
3. *Advantages of fusion* [Online; accessed 19. Nov. 2022]. Nov. 2022. https://www.iter.org/sci/Fusion.
4. Okada, S. & Momoshima, N. Overview of tritium: characteristics, sources, and problems. *Health Phys.* **65,** 595–609. ISSN: 0017-9078 (Dec. 1993).
5. *Fig. 1. Binding energy per nucleon B (Z , N) /A as a function of the...* [Online; accessed 22. Nov. 2022]. Nov. 2022. https://www.researchgate.net/figure/Binding-energy-per-nucleon-B-Z-N-A-as-a-function-of-the-mass-number_fig1_234065870.
6. Foh, S., Novil, M., Rockar, E. & Randolph, P. *Underground hydrogen storage. Final report. [Salt caverns, excavated caverns, aquifers and depleted fields]* [Online; accessed 19. Nov. 2022]. Dec. 1979.
7. G.Griffiths. *Tritium Storage for Fusion Energy* 2017.
8. Banos, A., Harker, N. J. & Scott, T. B. A review of uranium corrosion by hydrogen and the formation of uranium hydride. *Corros. Sci.* **136,** 129–147. ISSN: 0010-938X (May 2018).
9. Mulford, R. N. R., Ellinger, F. H. & Zachariasen, W. H. A New Form of Uranium Hydride1. *J. Am. Chem. Soc.* **76,** 297–298. ISSN: 0002-7863 (Jan. 1954).
10. Abraham, B. M. & Flotow, H. E. The Heats of Formation of Uranium Hydride, Uranium Deuteride and Uranium Tritide at 25°1. *J. Am. Chem. Soc.* **77,** 1446–1448. ISSN: 0002-7863 (Mar. 1955).

11. Rundle, R. E. The Structure of Uranium Hydride and Deuteride1. *J. Am. Chem. Soc.* **69,** 1719–1723. ISSN: 0002-7863 (July 1947).

12. Shugard, A. D., Tewell, C. R., Cowgill, D. F. & Kolasinski, R. D. *Uranium for hydrogen storage applications : a materials science perspective.* Aug. 2010.

13. Harker, R. M. The influence of oxide thickness on the early stages of the massive uranium–hydrogen reaction. *J. Alloys Compd.* **426,** 106–117. ISSN: 0925-8388 (Dec. 2006).

14. Wheeler, V. J. The diffusion and solubility of hydrogen in uranium dioxide single crystals. *J. Nucl. Mater.* **40,** 189–194. ISSN: 0022-3115 (Aug. 1971).

15. Teter, D. F., Hanrahan, R. J. & Wetteland, C. J. *Uranium Hydride Nucleation Kinetics: Effects of Oxide Thickness and Vacuum Outgassing* Mar. 2001.

16. Owen, L. W. & Scudamore, R. A. A microscope study of the initiation of the hydrogen-uranium reaction. *Corros. Sci.* **6,** 461–468. ISSN: 0010-938X (Jan. 1966).

17. Brill, M., Bloch, J. & Mintz, M. H. Experimental verification of the formal nucleation and growth rate equations – initial UH3 development on uranium surface. *J. Alloys Compd.* **266,** 180–185. ISSN: 0925-8388 (Feb. 1998).

18. Bloch, J. *et al.* The initial kinetics of uranium hydride formation studied by a hot-stage microscope technique. *Journal of the Less Common Metals* **103,** 163–171. ISSN: 0022-5088 (Nov. 1984).

19. Bloch, J. & Mintz, M. H. Kinetics and mechanism of the U-H reaction. *Journal of the Less Common Metals* **81,** 301–320. ISSN: 0022-5088 (Oct. 1981).

20. Kirkpatrick, J. R. & Condon, J. B. The linear solution for hydriding of uranium. *Journal of the Less Common Metals* **172-174,** 124–135. ISSN: 0022-5088 (Aug. 1991).

21. Condon, J. B. Calculated vs. experimental hydrogen reactions rates with uranium. *J. Phys. Chem.* **79,** 392–397. ISSN: 0022-3654 (Feb. 1975).

22. Kirkpatrick, J. R. Diffusion with chemical reaction and a moving boundary. *J. Phys. Chem.* **85,** 3444–3448. ISSN: 0022-3654 (Nov. 1981).

23. Loui, A., McCarrick, J. & McLean, W. Uranium hydride corrosion. I New insights into the Condon-Kirkpatrick model of uranium hydride formation rate. *Corros. Sci.* **191,** 109710. ISSN: 0010-938X (Oct. 2021).

24. Condon, J. B. Calculated vs. experimental hydrogen reactions rates with uranium. *J. Phys. Chem.* **79,** 392–397. ISSN: 0022-3654 (Feb. 1975).

25. Powell, G. L., Ceo, R. N., Harper, W. L. & Kirkpatrick, J. R. The Kinetics of the Hydriding of Uranium Metal II∗. *Z. Phys. Chem.* **181,** 275–282. ISSN: 2196-7156 (Jan. 1993).

26. E. Wicke, K. O. The uranium-hydrogen system and the kinetics of uranium hydride formation. *Z. Phys. Chem.* **31,** 222 (1962).

27. Bhattacharyya, R., Bandyopadhyay, D., Bhanja, K. & Mohan, S. Mathematical analysis of the hydrogen–uranium reaction using the shrinking core model for hydrogen storage application. *Int. J. Hydrogen Energy* **40,** 8917–8925. ISSN: 0360-3199 (Aug. 2015).

28. Mintz, M. H. & Bloch, J. Evaluation of the kinetics and mechanisms of hybriding reactions. *Prog. Solid State Chem.* **16,** 163–194. ISSN: 0079-6786 (Jan. 1985).

29. Kirkpatrick, J. R. & Dahl, C. A. *Review of Uranium Hydriding and Dehydriding Rate Models in GOTH()SNF for Spent Fuel MCO Calculations* [Online; accessed 23. Nov. 2022]. 2003.